Nigerian Journal of Technology (NIJOTECH)
Vol. 32. No. 2. July 2013, pp. 273-278

University of Nigeria, Nsukka, ISSN: 1115-8443
www.nijotech.com

CALCULATION OF COGGING TORQUE IN HYBRID STEPPING MOTORS

J. U. Agber
DEPARTMENT OF ELECTRICAL AND ELECTRONICS ENGINEERING, UNIVERSITY OF AGRICULTURE, MAKURDI, BENUE STATE. NIGERIA
e-mail: jonagber@yahoo.co.uk

Abstract:
When the windings of a hybrid stepping motor are unexcited the permanent magnet's flux produces cogging torque. This torque has both desirable and undesirable features depending on the application that the motor is put into. This paper formulates an analytical method for predicting cogging torque using measured flux-linkage data. It assumes a linear magnetic circuit, where the magnetic stored energy and coenergy are numerically equal. Cogging torque is calculated as the differential of the magnetic coenergy with respect to rotor angular position at constant rotor excitation. By representing the flux-linkage data with analytical function, the method produced results that compare favorably with laboratory test results.

Keywords: *Cogging torque, Detent torque, Stepping motor, Hybrid stepping motor, Incremental motion control.*

1. Introduction

The theory of stepping motors is beyond the scope of this paper and is adequately covered elsewhere [1, 2]. The characteristics of the hybrid stepping motor (HSM) can be analyzed using the equivalent circuit of the synchronous motor [3, 4]. Cogging torque is one of the characteristics displayed by HSM when the stator excitation is removed. It is called by various terms depending on how it works or what causes it, e.g. cogging torque, detent torque, salient-pole torque, reluctance torque, no-current torque, etc. It is desirable when it is used for detenting [5, 6] and undesirable when it causes torque and speed ripples [7 - 10]. It is therefore essential to have a reliable model which allows calculation of motor characteristics accurately. A lot of work has been done on prediction [4 - 6, 11 - 15] and reduction [7 - 10] of cogging torque in permanent magnet (PM) motors. Stuebig and Ponik [14] used the 2D finite element method (FEM) and flux-tube approach to calculate permeance for iron parts and air gap, while Deodhar et al [15] proposed the flux-magneto-motive force (mmf) method for estimating cogging torque of PM motors, while Kaiyuan [12] in furtherance with the flux-mmf method developed an analytical method that avoided the use of volume integral over the magnet. 2D and 3D FEM have also been used with either the virtual work method or Maxwell stress tensor [4, 11, 13, 14], but it has been noted [14] that 3D FEM is very time-consuming. Other methods proposed for reducing cogging torque include teeth pairing, magnet shaping and sizing, adding dummy stator slots, shifting of magnets and skewing [4, 11, 13, 16].

These methods although useful in resolving the particular problems being investigated, there is still room for improvement.

The aim of this paper is to develop an analytical method for predicting cogging torque/rotor angular position, $T_{cog}(\theta)$, characteristics using measured flux-linkage data. The flux-linkage data was measured from the conventional HSM and its wound-rotor equivalence. In the wound-rotor motor,

the PM was replaced with a wound soft-iron former and search coils were provided at the end cheeks of the former for measuring flux-linkage data.

2. Formulation of the Method

When the stator windings of a stationary HSM are unexcited and the flux is supplied solely by the PM, the air-gap flux, ϕ_{pm}, at a given rotor position, θ_k will depend only on the air-gap permeance, *P*, if the PM mmf, F_m, is assumed constant.

$$\phi_{pm}(\theta_k) = F_m P(\theta_k) \quad (1)$$

where $P(\theta_k)$ is the air gap permeance at rotor angular position θ_k.

If it is assumed that the flux-density on the face of the magnetized areas of the magnet is uniform and there is no saturation, the magnetic flux-density B_m can be estimated from the flux as:

$$B_m = \frac{\phi_{pm}(\theta_k)}{A_m} \quad (2)$$

where A_m is the cross-sectional area of the permanent magnet.

This method assumes a known B-H curve of the magnetized material from which the field intensity, H_m, can be found for subsequent calculation of F_m.

$$F_m = H_m l_c \quad (3)$$

where l_c = length of the mean magnetic path.

For a conservative electromagnetic system, the total system energy change due to angular displacement of rotor can be expressed as:

$$\Delta W_{elet} = \Delta W_{fld} + \Delta W_{mech} \quad (4)$$

where ΔW_{elect} is the electrical input energy supplied to the stator winding, ΔW_{fld} the variation of the stored magnetic energy due to the variation of the electrical energy and/or the mechanical work ΔW_{mech} given by the product of the torque and the angular displacement $\Delta\theta$. For cogging torque calculation, the electrical input power is zero; hence the magnetic energy is equal to and opposite the mechanical work [17]. For a specific position, this torque can be written as the partial derivative of magnetic energy with respect to the angular displacement θ:

$$T_{cog}(\theta) = -\frac{\partial W_{fld}(\theta)}{\partial \theta} \quad (5)$$

where

$$W_{fld}(\theta) = \int \phi(\theta) dF' \quad (6)$$

F' is a dummy variable of integration.

In a linear magnetic circuit, the stored magnetic energy and coenergy are numerically equal as shown in Figure 1. It follows that, for the rotor position θ_k, the magnetic energy can be written as:

$$W_{fld}(\theta_k) = 0.5 F \phi(\theta_k) \quad (7)$$

Equation (5) can be written as:

$$T_{cog}(\theta_k) = -0.5 F \frac{d\phi(\theta_k)}{d\theta} \quad (8)$$

Equation (8) is the general expression for $T_{cog}(\theta)$ using measured flux-linkage data.

3. Measurement of Flux-linkage Data

A static rig comprising a displacement transducer connected to one end of the shaft of the 1.8° stepping motor and on the other end, a torque transducer and a dynamometer. An analog flux meter is connected to either the series winding A-B' or the search coil on the soft-iron former and a torque meter is connected to the torque transducer. The displacement transducer is connected to the X-input of the X-Y plotter while both flux and torque meters are connected to the Y-input via a change-over switch.

Two methods of measuring the flux-linkage that produces cogging torque are described below.

3.1 Using stator pole windings

Figure 2 shows the cross-sectional view of the 1.8° HSM. Pole-pairs A-A' and C-C' carry the bifilar windings for phases A-A' and C-C', while pole-pairs B-B' and D-D' carry the windings for phases B-B' and phase D-D' (the windings for phases B-B' and D-D' windings are not shown in Figure 2). By connecting the phase windings of A-A' and phase B-B' in series, the winding phase A-B' now has twice the number of turns of a phase winding and covers all the four pole pairs. With this arrangement the variation of flux linking the four pole pairs can be observed.

The flux and torque measurements were done by displacing the rotor from the aligned position of pole-pair A-A' to misaligned position and back to the aligned position, covering a displacement of half a rotor tooth pitch or 3.6°. The forward and backward flux and torque curves were plotted. The curves were digitized and averaged to give the flux-linkage and cogging torque curves as shown in equations (9) and (10). The measured PM flux-linkage/rotor angular position is shown in Figure 3.

$$\phi_{cog}(\theta) = 0.5\{\phi_f(\theta) + \phi_b(\theta)\} \quad (9)$$

$$T_{cog}(\theta) = 0.5\{T_f(\theta) + T_b(\theta)\} \quad (10)$$

where the subscripts *f* and *b* denote forward and backward curves.

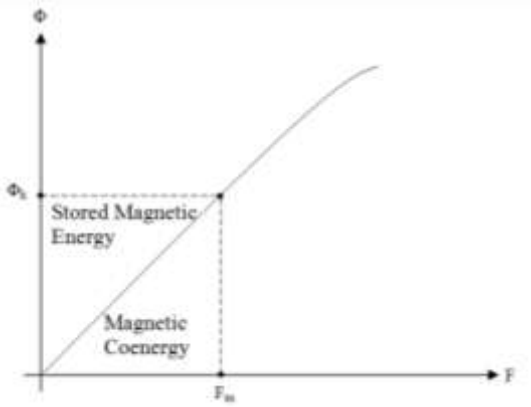

Figure 1. The graphical representation of stored magnetic energy and coenergy

3.2 Using rotor search coil

Since the wound-rotor motor is purely an experimental device, a soft-iron former, shown in Figure 4 was constructed to replace the PM and search coils were incorporated in the rotor assembly. This method of measuring flux-linkage data applies only to the wound-rotor or related motors, where search coils are fitted in the rotor. The test rig was similar to that described above, but in addition had a 24V dc supply and a rheostat for setting the wound rotor current.

The rotor search coils were connected through an analog flux meter to the Y-input of the X-Y plotter. When the rotor winding was energized, the rotor was moved, with respect to the reference pole-pair A-A', from the aligned position to the unaligned and back to the aligned. Two curves were plotted for both $\phi_{cog}(\theta)$ and $T_{cog}(\theta)$ at each excitation level. These curves were digitized and summed as shown in equations (9) and (10). The $\phi_{cog}(\theta)$ curves for the range of rotor excitation covered are shown in Figure 5.

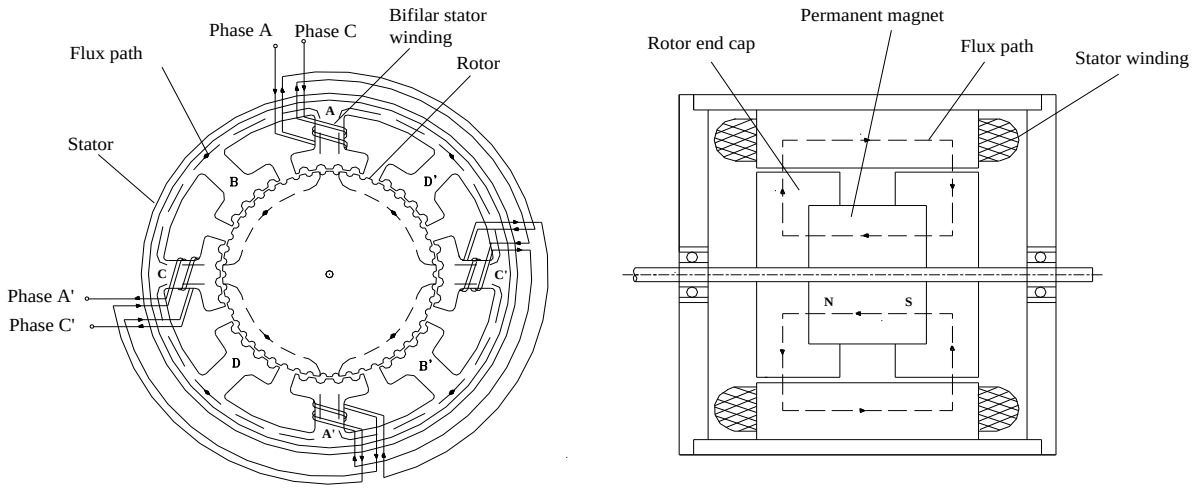

Figure 2. The cross-sectional views of the 1.8° hybrid stepping motor showing the PM flux and phase winding connections

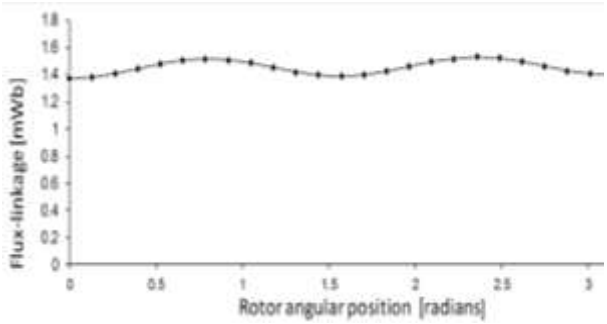

Figure 3: The permanent magnet flux-linkage measured from phase winding

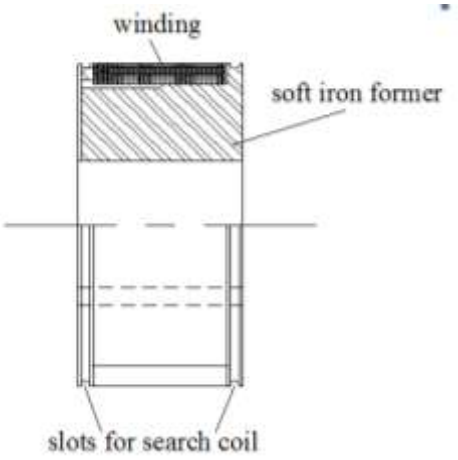

Figure 4: The soft iron former with winding to replace the permanent magnet in the rotor (soft iron material = MAXIMAG)

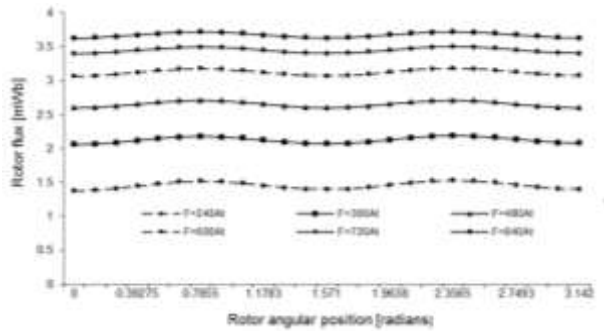

Figure 5: Rotor flux/rotor angular position curved at rotor mmf = 240At, 360At, 480At, 600At, 720At and 840At

4. Estimation of PM mmf

To use the present method on PM hybrid motors requires the estimation of the PM mmf. One way of doing this is to calculate the flux density from the open-circuit voltage, *V*, measured when the HSM was driven with the stator windings open-circuited [6].

$$B_{\max} = \frac{\sqrt{2}V}{2\pi f_r N A_m} \quad (11)$$

where *N* is the number of winding turns per phase, and f_r, frequency of the induced voltage.

B_{max} was used to find the magnetic field strength from the B-H curve of the magnetic material. The PM mmf is estimated using equation (3). For the wound-rotor motor, the mmf is simply the product *NI*, where *N* is the number of turns of rotor winding and *I* is the rotor excitation current.

5. Representation of Flux-linkage Data

This method involves the choice of an analytical function to represent the measured flux-linkage data. The function chosen must satisfy the following conditions:

a) It must provide continuous derivatives with respect to rotor angular position, θ.

b) It must be equal and opposite about the cogging torque zeroes ($N_r\theta$ = *0, π/4, π/2, 3π/4,* and π), where N_r is the number of rotor teeth.

c) It must be symmetrical about $N_r\theta$ = *π/8, 3π/8, 5π/8 and 7π/8.*

The fact that the $\phi_{cog}(\theta)$ curves obtained experimentally behave in a cosinusoidal manner for $0 \le N_r\theta \le \pi$, suggests that it can be approximated with cosine series in θ. Based on the requirements (a) to (c) above, a Fourier cosine series with only the fourth harmonic term can be used. To generalize the representation, the following Fourier cosine series is chosen:

$$f_{cog}(\theta) = A_0 + \sum_{k=1}^{n} A_k \cos(k N_r \theta) \quad (12)$$

where k = 1, 2, ….., *n* – an integer, the coefficient A_0 is for the dc offset in the flux-linkage data.

6. Calculation of cogging torque

Each curve, made up of 25 equally spaced θ-points, is approximated using the least error square routine [18]. With *n* = 6, the maximum average error per experimental point is 0.01mWb, which is better that 0.03% of the average flux-linkage at 600At. The calculated A_k coefficients are shown in Table 1.

Table 1. Coefficients generated from fitting the flux data measured at various rotor mmfs using the rotor search coil.

mmf / Coef	240At	360At	480 At	600 At	720 At	840 At
A_0	0.1457E 01	0.2126E 01	0.2654E 01	0.3125E 01	0.3452E 01	0.3675E 01
A_1	-0.1036E-01	-0.9136E-02	-0.3908E-03	-0.3730E-02	-0.3202E-02	-0.1928E-02
A_2	-0.2348E-03	0.7403E-03	-0.6023E-03	-0.1709E-03	-0.3273E-03	-0.1348E-04
A_3	-0.1347E-02	-0.1285E-02	-0.2306E-03	-0.3720E-03	-0.4964E-03	-0.3149E-03
A_4	-0.6765E-01	-0.5774E-01	-0.5460E-01	-0.5507E-01	-0.4947E-01	-0.4486E-01
A_5	-0.5340E-03	-0.4713E-03	-0.7732E-04	-0.2454E-03	-0.1260E-03	-0.1044E-03
A_6	-0.2485E-04	-0.2016E-03	-0.3185E-04	-0.1000E-03	-0.5612E-04	-0.1523E-04

Having established the function representing the flux data, equation (12), the expression for cogging torque, equation (8), demands the differential of the flux-linkage data with respect to rotor angular position θ.

Thus

$$\frac{df_{cog}(\theta)}{d\theta} = -N_r \sum_{k=1}^{6} k A_k \sin(k N_r \theta) \quad (13)$$

By substituting equation (13) into equation (8), an analytical expression for cogging torque/rotor angular position characteristics is obtained.

$$T_{cog}(\theta) = -0.5 N_r F \sum_{k=1}^{6} k A_k \sin(k N_r \theta) \quad (14)$$

Equation (14) is used to predict the cogging torque/rotor angular position and the results obtained are shown in Figure 6 for F = 240 and 600At. The maximum average error per experimental point is 0.048Nm, which is better that 1.4% of the peak cogging torque at 600At.

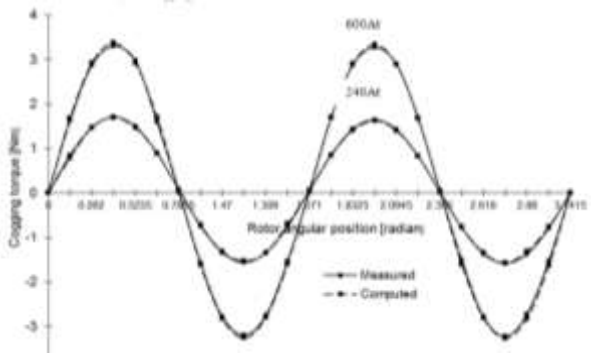

Figure 6: Measured and computed cogging torque at rotor mmf = 240At and 600At

7. Discussion

The presence of a PM in the rotor of the hybrid stepping motor enables the retention of rotor position whenever the supply to motor is turned off. This is due to the torque developed by the axial PM in the absence of stator excitation. An analytical method for estimating this torque was developed by Chai [3, 5] using the air-gap permeance at aligned and unaligned positions. The present method approximates the flux-linkage data measured from either the phase windings or rotor search coil with an analytical function. The function is integrated to yield the magnetic coenergy, which is differentiated to produce cogging torque. As can be seen, the chosen function fits the flux-linkage data and computes cogging torque/rotor angular position accurately. The good agreement between the theoretical and measured cogging torque/rotor angular position curves within the range of mmf covered shows that this method is capable of predicting cogging torque with high accuracy, thus confirming that an analytical method would give greater insight into the mechanism of cogging torque production [12].

Table 1 shows that the fourth harmonic term, A_4, is the dominant coefficient in the flux-linkage data. This is because the 1.8°, 40/50 teeth stepping motor has four cycles over one tooth pitch, i.e. the rotor teeth align with the stator teeth of each pole-pair over one tooth pitch. The dominance of the 4th harmonic term was earlier raised by Chai [5] that for a four phase, eight-pole PM stepping motor, the source of cogging torque is associated with the 4th harmonic component of the tooth permeance.

8. Conclusion

An analytical method for predicting cogging torque using measured flux-linkage data has been presented. Two methods of measuring the flux data that constitute cogging torque are shown. In the first method, the flux is measured from the phase windings connected in series. The second method uses search coils inserted in the rotor assembly. The flux-linkage measured using any of these methods is fitted to an analytical function, which is used for the prediction of cogging torque/rotor angular position characteristics. As it has been demonstrated, the measured and computed characteristics are reasonable and acceptable both in execution time and accuracy. This shows that the method is valid and can be used for the prediction of cogging torque/rotor angular position characteristics.

9. References

1. Kenjo, T. (1984) Stepping motors and their microprocessor controls. *Oxford monographs in Electrical Engineering*, Oxford, UK.
2. Acarnley, P. (2007) Stepping motors: A guide to theory and practice, *The Institution of Engineering and Technology*, 4th Edition, London, UK.
3. Chai, H. D. (1973) Magnetic circuit and formulation of static torque for single stack permanent-magnet and variable reluctance motors. *2nd Annual symposium on incremental motion control systems and devices*, University of Illinois, pp 120 – 140.
4. Hsiao, C.-Y., Yeh, S.-N. and Hwang, J.-C. (2011) A Novel Cogging Torque Simulation Method for Permanent-Magnet Synchronous Machines, *MDPI Journal of Energies,* Vol. 4, pp 2166 – 2179. www.mdpi.com/journal/energies
5. Chai, H. D. (1984) Cogging torque of permanent-magnet step motors. *13th Annual symposium on incremental motion control systems and devices*, University of Illinois, pp 163 – 166.
6. Agber, J. U. (1985) Hybrid stepping motors with multiple-teeth per pole. *Unpublished PhD thesis*, University of Newcastle Upon Tyne, UK.
7. Dosiek, L. and Pillay, P. (2007) Cogging Torque Reduction in Permanent Magnet Machines, *IEEE Transactions on Industrial Applications,* Vol. 43, No. 6.
8. Muljadi, E. and Green, J. (2002) Cogging Torque Reduction in a Permanent Magnet Wind Turbine Generator, *21st American Society of Mechanical Engineers Wind Energy Symposium Rano, Nevada*, January 14 – 17.
9. Wang, Y., Wang, X., Qiao, D., Pei, Y., and Jung, S.-Y. (2011) Reducing Cogging Torque in Surface-mounted Permanent-Magnet by Nonuniformly Distributed Teeth Method, *IEEE Transaction on Magnetics,* Vol. 47, pp 2231 – 2239.
10. Wang, Y., Jin, M. J., Fei, W. Z. and Shen, J. X. (2010) Cogging Torque Reduction in Permanent Magnet Flux-switching Machines by Rotor Teeth Axial Pairing, *IET Electric Power Application,* Vol. 4, pp 500 – 506.
11. Tudorache, T., Melcescu, L., Popescu, M. and Cistelecan, M (2008), M. Finite Element Analysis of Cogging Torque in low Speed Permanent Magnets Wind Generators, *Renewable Energy and Power Quality Journal,* No. 6.
12. Kaiyuan, L., Rasmussen, O. and Ritchie, E. (2006) An Analytical Equation for Cogging Torque Calculation in Permanent Magnet Motors, *17th International Conference on Electrical Machines,* Chania, Kreta, Greece.
13. Lee, J.-J., Kwon, S.-O., Hong, J.-P. and Ha, K.-H. (2009) Cogging Torque Analysis of the PMSM for High Performance Electrical Motor Considering Magnetic Anisotropy of Electrical Steel, *World Electric Vehicle Journal,* Vol. 3.
14. Stuebig, C.; and Ponick, B. (2008) Determination of Air Gap Permeances of Hybrid Stepping Motors for Calculation of Motor Behaviour, *Proc. International Conference on Electrical Machines*, Paper ID 1239.
15. Deodhar, R. P., Staton, D. A., Jahns, T. M. and Miller, T. J. E. (1996) Prediction of Cogging Torque using the Flux-MMF Diagram Technique, *IEEE Transactions on Industrial Applications*, Vol. 32, pp. 569 – 576.
16. Zhu, Z. Q. (2000) Influence of Design Parameters on Cogging Torque in Permanent Magnet Machines, *IEEE Transactions on Energy Conversion.* Vol. 15, No. 4.
17. Fitzgerald, A. E., Kingsley, C., and Umans, S. D. (2003). *Electric Machinery*. Mc-Graw Hill Higher Education, 6th Edition, Tokyo, pp 129 – 155
18. NAG Toolbox for MATLAB (2011), *Numerical Algorithms Group (NAG), (Release 5.3)*, W.lkinson House, Oxford, UK.